Charge Density Wave Dislocation as Revealed by Coherent X-Ray Diffraction

D. Le Bolloc'h,[1] S. Ravy,[2] J. Dumas,[3] J. Marcus,[3] F. Livet,[4] C. Detlefs,[5] F. Yakhou,[5] and L. Paolasini[5]

[1]*Laboratoire de Physique des Solides (CNRS-UMR 8502), Bâtiment 510, Université Paris-sud, 91405 Orsay cedex, France*
[2]*Synchrotron SOLEIL, L'Orme des merisiers, Saint-Aubin BP 48, 91192 Gif-sur-Yvette cedex, France*
[3]*Laboratoire d'Étude des Propriétés Électroniques des Solides-CNRS, BP 166, 38042 Grenoble cedex, France*
[4]*LTPCM (CNRS-UMR 5614), ENSEEG-Domaine Universitaire, BP 75, 38402 Saint Martin d'Hères cedex, France*
[5]*European Synchrotron Radiation Facility, BP 220, 38043 Grenoble cedex, France*

(Received 11 April 2005; published 7 September 2005)

Coherent x-ray diffraction experiments have been performed on high quality crystals of the charge density wave (CDW) system $K_{0.3}MoO_3$. The satellite reflections associated with the CDW have been measured as a function of the 20-μm-diameter beam position. For some positions, regular fringes have been observed. We show that this observation is consistent with the presence of a single CDW dislocation. Beyond charge density wave systems, this experiment shows that coherent x-ray diffraction is a suitable tool to probe topological defects embedded in the bulk.

DOI: 10.1103/PhysRevLett.95.116401 PACS numbers: 71.45.Lr, 61.10.−i

The richness of charge density wave (CDW) properties is directly related to the one-dimensional (1D) character of their electronic structure. Upon cooling, the quasi-1D electron system undergoes a 3D modulation of the electronic density, at twice the Fermi wave vector $2k_F$, associated with a periodic distortion of the host lattice [1,2]. The CDW ground state resulting from this instability is a typical example of electronic crystal. This crystal can slide as a whole for an electric field larger than a threshold, whose existence is related to the pinning of the CDW on defects.

As any crystal, a CDW is elastic and can exhibit intrinsic defects like dislocations. Detailed knowledge of these defects is essential to understand the CDW dynamics as first suggested in Ref. [3]. Indeed, the conversion of free carriers into condensed electrons near contacts [4–7] requires one to create or destroy CDW phase fronts by dislocation climbing [5]. The variations of the CDW wave vector with temperature, or the narrow band noise generated by the CDW sliding, are other phenomena interpreted as due to dislocations [4,5].

Although CDW dislocations are structural features, such defects have never been directly observed in electronic crystals by diffraction methods [8], even though indirect evidence of CDW dislocations close to contacts have been reported [9]. The goal of this Letter is to show that coherent x-ray diffraction is a suitable tool to probe phase field deformations induced by dislocations.

By diffraction, the periodic lattice distortion $\mathbf{u}(\mathbf{r}) = \mathbf{u}_0 \cos[\mathbf{q}_c \cdot \mathbf{r} + \Phi(\mathbf{r})]$ associated with the CDW gives rise to satellite reflections located at $\pm\mathbf{q}_c$ around each fundamental Bragg reflection. In *usual* diffraction experiments, the low degree of coherence of the beam makes the satellite intensity proportional to the Fourier transform squared of the *space average* $\langle u(0)u(\mathbf{r})\rangle$. The corresponding satellite *smooth* profiles can be explicitly calculated from, e.g., phase-only weak pinning models based on the Fukuyama-Lee-Rice Hamiltonian [3,10,11]. From an experimental point of view, the behavior of the phase $\Phi(\mathbf{r})$ through the phase-phase correlation function $\langle\Phi(\mathbf{r})\Phi(0)\rangle$ is difficult to obtain from the satellite profiles because domains are often close to the micrometer size in pure systems and diffraction peaks are thus resolution limited. In doped systems, in which reflections are broad enough, the experimental profiles are consistent with either *weak pinning* situations, in which the CDW domains pin as a whole [12,13], or *strong pinning* ones, in which each impurity pins the CDW phase [14,15].

The coherent diffraction of disordered systems no longer leads to smooth diffraction features but to speckle patterns, which are related to the exact disorder configuration probed by the x-ray beam. Indeed, a first coherent diffraction experiment performed on $NbSe_3$ clearly showed a typical speckle pattern [16]. In this Letter, we report on the coherent diffraction in the CDW state of the *pure,* high quality, molybdenum blue bronze $K_{0.3}MoO_3$ sample [2] (see Fig. 1). We show that it is consistent with the presence of a single CDW dislocation embedded in the bulk.

$K_{0.3}MoO_3$ is made of clusters of 10 MoO_6 octahedra forming chains along the [010] direction and layers along the [102] direction. It crystallizes in the monoclinic $C2/m$ space group with the cell parameters $a = 18.25$ Å, $b = 7.56$ Å, $c = 9.885$ Å, and $\beta = 117.5°$. This structure is conveniently described using the pseudo-orthogonal basis of reciprocal vectors $\mathbf{b}^*$, along the chain's direction, $2\mathbf{a}^* + \mathbf{c}^*(\sim\mathbf{a} + 2\mathbf{c})$, close to the perpendicular direction within the layer, and $2\mathbf{a}^* - \mathbf{c}^*$, perpendicular to the layers. The satellite reflections are found at the $(0, 1 - 2k_F, \overline{0.5})$ reduced wave vector, where $2k_F$ is equal to the incommensurate value $0.748 \pm 0.001b^*$ at 15 K [17]. This leads to define $\mathbf{q}_c = (1, 2k_F, \overline{0.5})$ as the CDW wave vector normal to the wave fronts. Note that the CDW reduced wave vector $\mathbf{q}_c$ is not parallel to the chains direction $\mathbf{b}^*$, as it is usually assumed in theoretical works (see Fig. 2).

The $0.5 \times 2 \times 0.2$ mm^3 sample was mounted in an Orange Cryostat at the ID20 beam line at the ESRF and

cooled down to 75 K. The sample was initially aligned with the $\mathbf{b}^*$ axis vertical, and the $2\mathbf{a}^* - \mathbf{c}^*$ axis in the horizontal scattering plane. In order to get a good transverse coherence of the 7.5 keV beam ($\lambda = 1.65$ Å), and to get rid of the distortions of the source by the optics, we used a set of slits (20 μm $\times$ 20 μm) as a virtual source 3 m before the sample. An approximate degree of coherence of 60%–70% was achieved by using a $d = 20$ μm diameter pinhole as close as possible to the sample (12 cm). The patterns were recorded on a direct illuminated CCD camera (20 μm $\times$ 20 μm pixel size) located 1.73 m from the sample position. The data were analyzed by a DROPLET algorithm [18].

The experiment consisted in recording the 2D diffraction patterns of the $\mathbf{Q_s} = (5, \bar{1}, \bar{3}) + \mathbf{q_c}$ reflection for different beam positions on the sample. Because of the experimental geometry, the 2D reciprocal plane corresponds to the $(\mathbf{b}^*, \mathbf{t}^*)$ plane, where $\mathbf{t}^*$ is the direction tilted at 19.5° from the $2\mathbf{a}^* - \mathbf{c}^*$ direction (see Fig. 3). For most of the positions, the pattern exhibited a sharp component only [see Fig. 1(a)], far from typical speckle patterns of disordered systems. The spot is almost circular ($\approx$50 μm in FWHM) and slightly elongated along $\mathbf{t}^*$. By translating vertically the sample by 20 μm steps over 2 mm, the profile did not display any speckle for most of the cases. For some beam positions on the sample, however, regular fringes appeared, in the $\mathbf{t}^*$ direction only [see Fig. 1(b)]. The profile of the fringes was very sensitive to the incident angle θ_i, whereas the profile along $\mathbf{b}^*$ did not depend on θ_i and never displayed any fringe. Similar diffraction patterns were observed in another sample [19] and no fringe was ever observed on the $(6, 0, \bar{3})$ fundamental Bragg reflection [see Fig. 1(c)].

Let us discuss the size of the diffraction peak in Fig. 1(a). Because the penetration length ($\mu^{-1} = 18$ μm) and the pinhole size ($d = 20$ μm) are large, we are not here in the pure Fraunhofer regime [20]. In this

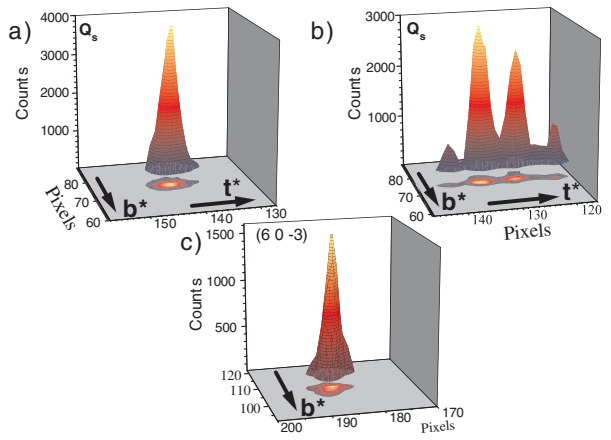

FIG. 1 (color online). Two-dimensional diffraction patterns of the $\mathbf{Q_s}$ satellite reflection in the $(\mathbf{b}^*, \mathbf{t}^*)$ plane (see text) for two different beam positions at $T = 75$ K: (a) 20 s, and (b) 100 s of exposure times. (c) Typical 2D diffraction pattern of the (6 0 $-$3) fundamental Bragg reflection.

intermediate regime, the diffracted beam in the two transverse directions ($\mathbf{b}^*$ and $2\mathbf{a}^* + \mathbf{c}^*$) is driven by the pinhole size [21]. The width along the radial direction $2\mathbf{a}^* - \mathbf{c}^*$ is, however, larger and driven by μ and the longitudinal coherence length ξ_L given by the double Si monochromator of the beam line [22]. This leads to a cigarlike profile, elongated along the radial direction. This is why the experimental profile appears slightly elongated along the direction $\mathbf{t}^*$.

The contrast of fringes in Fig. 1(b) is related to the maximum path length difference Δ, which is usually limited by the penetration length μ and the diffraction angle θ: $\Delta = 2\ \mu^{-1}\sin^2\theta$. In a more general case, when the scattering wave vector is inclined of an angle α with respect to the surface, the maximum path length difference reads

$$\Delta = 2\mu^{-1}\frac{\sin\theta_i \sin\theta_f}{\cos\alpha}. \quad (1)$$

In order to reduce Δ, the most intense low-angle superstructure reflection $\mathbf{Q}_s$ at the incident angle $\theta_i = 12.6°$ and exit angle $\theta_f = 26.4°$ was studied (see Fig. 3). In this geometry, Δ remains larger than ξ_L ($\Delta = 3.5$ μm and $\xi_L = \frac{\lambda^2}{\Delta\lambda} = 1.4$ μm). This effect reduces the contrast of fringes along the radial direction $2\mathbf{a}^* - \mathbf{c}^*$. However, the contrast in Fig. 1(b) is still strong because the direction of measurement $\mathbf{t}^*$ is tilted at $\theta = 19.5°$ from the radial direction [see Fig. 3(b)].

The presence of regular fringes in Fig. 1(b) could be due to the diffraction of an isolated domain smaller than the transverse coherent length of the beam. Such a truncation effect, however, leads to fringes whose intensity is weak and visible on log scales only (see, for example, the diffraction of slits or nanocrystals [23]). Those fringes cannot be due to the mosaicity of the CDW either, because the 2D diffraction patterns were obtained for fixed θ. The fringes observed here are thus due to interference effects induced by localized phase field deformation of the CDW. In the following, we show that the original diffraction pattern of Fig. 1(b) is consistent with a single screwlike dislocation of the CDW.

The space averaged x-ray diffraction pattern in the presence of several dislocations has been considered in a number of theoretical works (see, for example, [24]). We treat here the case of the coherent diffraction of a dislocation and its associated phase field deformation.

As in any elastic medium, simple cases of screw and edge dislocations can be considered, given that the 1D character of CDW requires a Burgers vector parallel to $\mathbf{q_c}$ [6]. Restricting ourselves to 1D perfect dislocation lines, we apply the basic theory of elasticity [3,6,25]. The phase $\Phi(\mathbf{r})$ has to fulfill the differential equation at equilibrium: $K_x(\frac{d^2\Phi}{d^2x}) + K_y(\frac{d^2\Phi}{d^2y}) + K_z(\frac{d^2\Phi}{d^2z}) = 0$, where K_i are the classical elastic constants in the three directions i. Dilatation and compression of the CDW along the $2k_F$ direction ($\mathbf{b}^*$) produce an excess or a default of charge, expensive in terms of Coulomb energy, while shears per-

pendicular to $\mathbf{b}^*$ are neutral. The elastic constants K_i are thus expected to be strongly anisotropic in a CDW system, as confirmed by inelastic scattering measurements on blue bronzes [26,27]: $\frac{K_{b^*}}{100} = \frac{K_{2a^*+c^*}}{19.4} = K_{2a^*-c^*}$ and $K_{b^*} = 10^5$ eV cm^{-1}.

The absence of fringe along $\mathbf{b}^*$ and the knowledge of the elastic constants reduce the number of solutions to (i) the screwlike dislocation where the Burgers vector is $\mathbf{q_c}$ and running along the $\mathbf{b}^*$ direction $[\Phi = \tan^{-1}(\sqrt{\frac{K_x}{K_z}}\frac{z}{x})]$ and (ii) the edge dislocation whose line is along $2\mathbf{a}^* - c^*$ $[\Phi = \tan^{-1}(\sqrt{\frac{K_x}{K_y}}\frac{y}{x})]$. Although the solution of the edge dislocation cannot be excluded, the screwlike dislocation has been considered only in the following, fitting the experimental data with a better accuracy. Because the CDW wave vector $\mathbf{q_c}$ is not parallel to the chain's axis, it corresponds to a mixed dislocation, running in the chain's direction (see Fig. 2). Remarkably, this dislocation introduces no compression or dilatation of the CDW along $\mathbf{b}^*$.

The corresponding diffraction pattern around the satellite position $\mathbf{Q_s}$ is displayed in Fig. 3. The experimental elastic constants given above have been used. The diffraction pattern is characterized by a minimum of intensity at $\mathbf{Q_s}$, whereas a maximum is expected in the case of a perfect CDW. No fringe appears along $\mathbf{b}^*$ in agreement with the experiment, and the main fringes are observed along the soft direction $2\mathbf{a}^* - \mathbf{c}^*$. Our CCD camera cuts the $(2\mathbf{a}^* - \mathbf{c}^*; 2\mathbf{a}^* + \mathbf{c}^*)$ plane along $\mathbf{t}^*$. By slightly changing the incident angle θ_i, the section is translated along the arrow indicated in Fig. 3(b). This explains the sensitivity of the diffraction pattern with the incident angle. Since this dislocation affects the CDW modulation only and not the host lattice, it induces no change on the fundamental Bragg reflections.

The profile of fringes depends on the location of the screwlike dislocation in the probed volume. In depth, one can estimate from simulations [28] that the dislocation line has to be located between $\frac{\mu^{-1}}{5}$ (=3.6 μm) and $\frac{\mu^{-1}}{3}$ (=6 μm) from the surface to be visible. Along $\mathbf{b}^*$, the dislocation has to be located at less than $\frac{d}{4}$ (=5 μm) from the center of the beam. The simulated diffraction profile of this screwlike dislocation located at $\frac{\mu^{-1}}{3.6}$ from the surface properly fits the experimental data (see Fig. 4).

Althrough fringes are observed along $\mathbf{t}^*$ for given locations in the sample, no fringe was ever observed along $\mathbf{b}^*$, whatever the beam position or/and the incident angle. This is an indication that the CDW remains globally coherent along $\mathbf{b}^*$, over very large distances (over millimeters). Note here that we are not sensitive to 2π solitons or to slow variations of the modulation.

We took into account only a single 1D perfect dislocation line without considering several dislocations or more complex topological defects as dislocation loops. However, the original diffraction pattern of Fig. 1(b), especially the small number of fringes, limits significantly the number of solutions. For example, the presence of several dislocations would imply many more fringes and loop dislocations additional fringes along $\mathbf{b}^*$. Moreover, since screw dislocations involve shears, they have smaller energies than edge ones, which involve compression and dilatation along the $2k_F$ direction $\mathbf{b}^*$. The presence of CDW screwlike dislocations is thus expected from theoretical arguments [6].

In conclusion, we report here the first direct observation of a topological defect of an electronic crystal, embedded

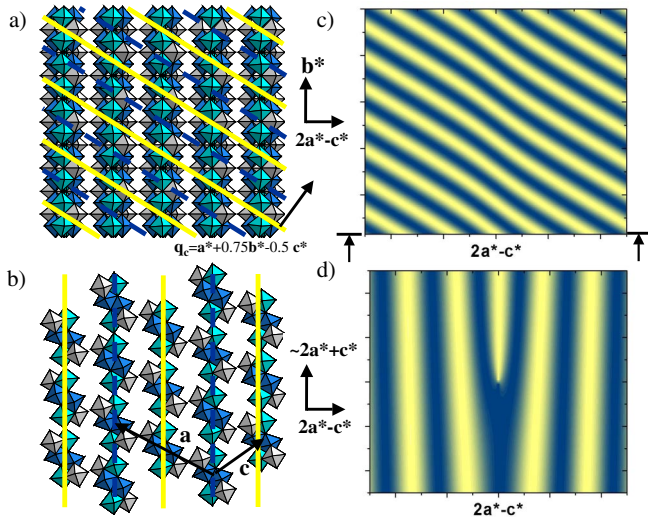

FIG. 2 (color online). Schematic representation of the CDW phase fronts in the blue bronze in the (a) $(2\mathbf{a}^* - \mathbf{c}^*; \mathbf{b}^*)$ plane and (b) $(2\mathbf{a}^* - \mathbf{c}^*; 2\mathbf{a}^* + \mathbf{c}^*)$ plane. Only Mo octahedra are represented. Light and dark straight lines represent the 0 and π constant phases of the CDW modulation. Sections of the CDW screwlike dislocation described in the text are displayed in (c) and (d). The size of the planes has been increased by a factor of 2. The appearance of an edge dislocation in (d) is due to the mixed character of the dislocation (see text).

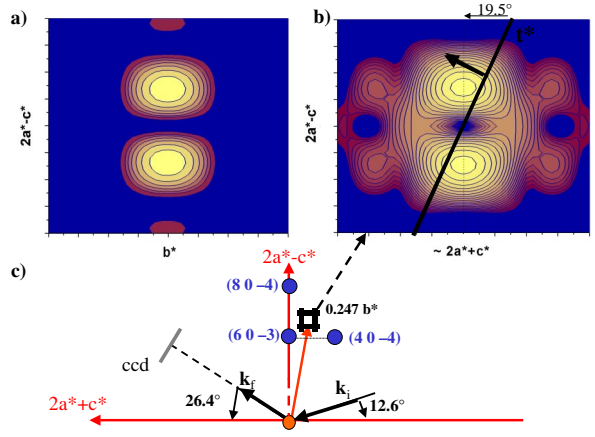

FIG. 3 (color online). Simulated diffraction patterns around the satellite reflection $\mathbf{Q_s}$ of the screwlike dislocation described in Fig. 2 in (a) the $(\mathbf{b}^*; 2\mathbf{a}^* - \mathbf{c}^*)$ and (b) $(2\mathbf{a}^* + \mathbf{c}^*; 2\mathbf{a}^* - \mathbf{c}^*)$ planes. The black line represents the measured section of the reciprocal lattice. (c) Schematic representation of the diffraction geometry. Note that the fundamental reflections and $\mathbf{Q}_s$ are not in the same planes (not in scale).

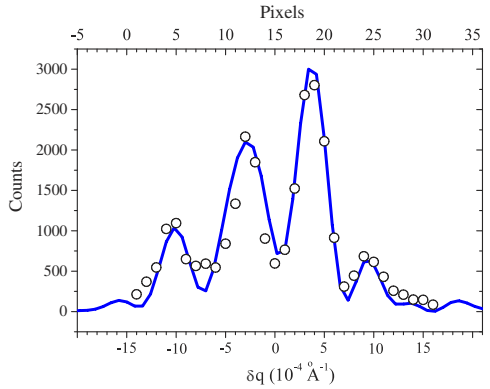

FIG. 4 (color online). Experimental profile of Fig. 1(b) along $\mathbf{t}^*$ (open cercles) and the simulated diffraction of the screwlike dislocation described in Fig. 2 (straight line).

in the bulk, by using the properties of a coherent x-ray beam. This observation is particularly important in the case of CDW systems where the intrinsic defects are the cornerstone of a number of physical phenomena. Beyond CDW systems, this study shows that coherent x-ray diffraction is well suited to probe any phase field deformation in the bulk, in nearly perfect lattices.

The authors acknowledge M. Sutton, J. P. Pouget, S. Brazovskii, N. Kirova, and C. Schlenker for helpful discussions and P. Van den Linden for his technical support.

[1] R. E Peierls, *Quantum Theory of Solids* (Oxford University Press, New York, 1955), p. 108; H. Frohlich, Proc. R. Soc. A **223**, 296 (1954).
[2] For reviews on CDW systems, see *Low Dimensional Electronic Properties of Molybdenum Bronzes and Oxides*, edited by C. Schlenker (Klüwer Academic, Dordrecht, 1989).
[3] P. A. Lee and T. M. Rice, Phys. Rev. B **19**, 3970 (1979).
[4] L. P. Gor'kov, Pis'ma Zh. Eksp. Teor. Fiz. **38**, 76 (1983); [Sov. Phys. JETP **38**, 87 (1983)].
[5] N. P. Ong, G. Verma, and K. Maki, Phys. Rev. Lett. **52**, 663 (1984); N. P. Ong and K. Maki, Phys. Rev. B **32**, 6582 (1985); S. Ramakrishna, Phys. Rev. B **48**, 5025 (1993).
[6] D. Feinberg and J. Friedel, in [2], p. 407; D. Feinberg and J. Friedel, J. Phys. II (France) **49**, 485 (1988).
[7] S. A. Brazovskii and S. I. Matvenko, Sov. Phys. JETP **72**, 860 (1991).
[8] In 2D CDW systems like 2H-$TaSe_2$, direct observation of discommensurations and their associated dislocations has been reported by using dark field electron microscopy: C. H. Chen, J. B. Gibson, and R. M. Fleming, Phys. Rev. Lett. **47**, 723 (1981); K. K. Fung, S. McKerman, J. W. Steeds, and J. A. Wilson, J. Phys. C **14**, 5417 (1981). Properties of these dislocations are also discussed in [25], but these topological defects are different from the intrinsic CDW dislocations described here.
[9] S. Brazovskii, N. Kirova, H. Requardt, F. Ya. Nad, P. Monceau, R. Currat, J. E. Lorenzo, G. Grübel, and Ch. Vettier, Phys. Rev. B **61**, 10 640 (2000); D. Rideau, O. Monceau, R. Currat, H. Requard, F. Nad, J. E. Lorenzo, S. Brazovski, C. Detlefs, and G. Grübel, Europhys. Lett. **56**, 289 (2001).
[10] H. Fukuyama and P. A. Lee, Phys. Rev. B **17**, 535 (1978).
[11] A. Rosso and T. Giamarchi, Phys. Rev. B **68**, 140201(R) (2003); **70**, 224204 (2004).
[12] S. M. DeLand, G. Mozurkewich, and L. D. Chapman, Phys. Rev. Lett. **66**, 2026 (1991).
[13] D. DiCarlo, R. E. Thorne, E. Sweetland, M. Sutton, and J. D. Brock, Phys. Rev. B **50**, 8288 (1994).
[14] S. Ravy, J.-P. Pouget, and R. Comès, J. Phys. I (France) **2**, 1173 (1992).
[15] S. Rouzière, S. Ravy, J.-P. Pouget, and S. Brazovskii, Phys. Rev. B **62**, R16 231 (2000).
[16] M. Sutton, Y. Li, J. D. Brock, and R. E. Thorne, J. Phys. IV (France) **12**, Pr9-3 (2002).
[17] J.-P. Pouget, C. Noguera, A. H. Moudden, and R. Moret, J. Phys. (Paris) **46**, 1731 (1985); J.-P. Pouget, in Ref. [2], p. 87.
[18] F. Livet, F. Bley, M. Sutton, J. Mainville, E. Geissler, G. Dolino, and R. Caudron, Nucl. Instrum. Methods Phys. Res., Sect. A **451**, 596 (2000).
[19] See ESRF Report No. hs1284, 2002.
[20] The Fraunhofer regime is reached for distances much larger than $\frac{d^2}{\lambda}$: S. K. Sinha, M. Tolan, and A. Gibaud, Phys. Rev. B **57**, 2740 (1998); M. Born and E. Wolf, *Principles of Optics* (Pergamon Press, Oxford, 1980).
[21] In first approximation, the sample reflects the image of the pinhole: along b^*, the size of the diffracted beam just after the sample is close to 20 μm and reaches 50 μm at the detector position. Along $2a^* + c^*$, the diffracted beam is elongated due to asymmetic geometry (38 μm after the sample) and remains almost parallel until the detector position.
[22] In the Fraunhofer regime, the width of the Lorentz profile along the radial direction due to μ only would read $\delta q = \frac{\mu}{2}[\frac{1}{\sin\theta_i} + \frac{1}{\sin\theta_f}] = 1.9 \times 10^{-5}$ Å^{-1}.
[23] D. Le Bolloc'h, F. Livet, F. Bley, T. Schulli, M. Veron, and T. H. Metzger, J. Synchrotron Radiat. **9**, 258 (2002); G. J. Williams, M. A. Pfeifer, I. A. Vartanyants, and I. K. Robinson, Phys. Rev. Lett. **90**, 175501 (2003).
[24] M. A. Krivoglaz, *Theory of X-ray and Thermal Neutrons Scattering by Real Crystals* (Plenum Press, New York, 1969).
[25] J. Dumas and D. Feinberg, Europhys. Lett. **2**, 555 (1986).
[26] B. Hennion, J.-P. Pouget, and M. Sato, Phys. Rev. Lett. **68**, 2374 (1992); J.-P. Pouget, B. Hennion, C. Escribe-Fillipini, and N. Sato, Phys. Rev. B **43**, 8421 (1991).
[27] S. Ravy, H. Requart, D. Le Bolloc'h, P. Foury-Leleykian, J.-P. Pouget, R. Currat, and P. Monceau, Phys. Rev. B **69**, 115113 (2004).
[28] The simulations consist in 3D Fourier transform of the CDW modulation considered as a continuous function.